Properties of GaP(001) surfaces treated in aqueous HF solutions

Hiroaki Morota and Sadao Adachi
Department of Electronic Engineering, Faculty of Engineering, Gunma University, Kiryu-shi, Gunma 376-8515, Japan

(Received 23 January 2007; accepted 2 April 2007; published online 7 June 2007)

Chemically cleaned GaP(001) surfaces in aqueous HF solutions have been studied using spectroscopic ellipsometry (SE), *ex situ* atomic force microscopy (AFM), x-ray photoelectron spectroscopy (XPS), wettability, and photoluminescence (PL) measurements. The SE data clearly indicate that the solutions cause removal of the native oxide film immediately upon immersing the sample ($\leq$1 min). The SE data, however, suggest that the native oxide film cannot be completely etch-removed. This is due to the fact that as soon as the etched sample is exposed to air, the oxide starts to regrow. The SE estimated roughness is ~1 nm, while the AFM roughness value is ~0.3 nm. The XPS spectra confirm the removal of the native oxide and also the presence of regrown oxide on the HF-etched GaP surface. The wettability measurements indicate that the HF-cleaned surface is hydrophobic, which is in direct contrast to those obtained from alkaline-cleaned surfaces (hydrophilic). A slight increase in the PL intensity is also observed after etching in aqueous HF solutions. © *2007 American Institute of Physics*. [DOI: 10.1063/1.2737781]

I. INTRODUCTION

Gallium phosphide (GaP) is one of the most important III−V semiconductors because of its applications to optoelectronic and high-temperature electronic transport devices. Because of its highly reactive nature, the GaP surface is easily oxidized in room-temperature air with the formation of a native oxide film several nanometers thick. A clean material surface is absolutely essential for various semiconductor device techniques.

Several surface cleaning techniques are available for the III-V semiconductors.[1–3] Among them, chemical cleaning is the simplest and easiest to control and has been widely applied to GaAs,[2–13] InP,[3,11,14–16] and GaP.[17,18] The chemicals used in these studies are mainly acidic (HCl, HF, H_2SO_4/H_2O_2, etc.) and alkaline (KOH, NH_4OH, etc.) solutions.

A useful guide to references on wet chemical cleaning has been given by Clawson[19] who presented some of the works done on III-V semiconductors. However, the literature discussing on the surface cleaning of GaP is still limited[17,18]: only reports have been published on the chemical cleaning of the GaP surface in acidic (HCl) (Ref. 17) and alkaline (KOH, NH_4OH) (Ref. 18) solutions. No cleaning study in acidic HF solution has been performed to date. In silicon technology, HF cleaning is well known to result in the removal of the native oxide and leaves behind stable silicon surfaces terminated by atomic hydrogen.

In this article, we report on the chemical cleaning effects of GaP(001) surfaces in HF solution studied using spectroscopic ellipsometry (SE), *ex situ* atomic force microscopy (AFM), x-ray photoelectron spectroscopy (XPS), wettability, and photoluminescence (PL) spectroscopy. SE is a highly surface-sensitive technique to detect not only submonolayer coverage of a surface by adsorbed species, but also the surface roughness of its size smaller than the wavelength of light.[20] An AFM is used to independently assess surface morphology changes that result from HF etching and that enter into our optical modeling using SE data. An XPS is also used to give an overview of the core-level XPS lines on the HF-treated surfaces.

II. EXPERIMENT

The GaP samples used in this study were *n*-type Te-doped (001) wafers with resistivity ~0.15 Ω cm. The samples were first degreased with organic solvents in an ultrasonic bath and then rinsed with de-ionized water. No further cleaning of the sample surface was performed. The sample surfaces to be studied were, then, covered with a ~2-nm-thick native oxide film. Note that this value was determined by SE and thus the effective thickness, modeled as an equivalent dielectric layer of the GaP oxide, not the actual one.

The concentration of the HF solution was 1 wt % and 50 wt %. Etching experiments were performed at room temperature and in room light. After the chemical treatment, the samples were rinsed in de-ionized water.

The HF-cleaned samples were immediately characterized by SE, AFM, XPS, wettability, and PL measurements. The SE instrument used was of the rotating-analyzer type (DVA-36VW-A, Mizojiri Optical, Co., Ltd.). A 150-W xenon lamp was used as the light source. The SE measurement was performed in the 2.0–5.2-eV photon-energy range at 300 K. The angle of incidence and the polarizer azimuth were set at 70° and 45°, respectively.

The microscopic structures of the HF-cleaned GaP(001) surfaces were examined by the AFM (Digital Instruments Nanoscope III) in the tapping mode and in the repulsive force regime. The XPS measurements were performed with an ULVAC-PHI Model 5600 spectrometer equipped with an Mg $K\alpha$ (1253.6 eV) line as an x-ray source. The take-off angle of photoelectrons was 45°. Gallium 2*p* and P 2*p* core levels were mainly examined. Wettability measurements

0021-8979/2007/101(11)/113518/6/$23.00 © 2007 American Institute of Physics

Downloaded 11 Oct 2007 to 210.151.113.98. Redistribution subject to AIP license or copyright, see http://jap.aip.org/jap/copyright.jsp

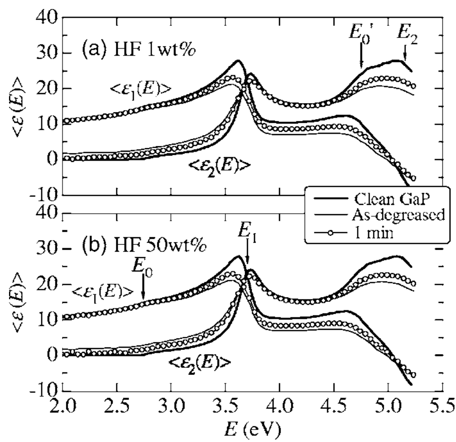

FIG. 1. Real $[\langle\varepsilon_1(E)\rangle]$ and imaginary $[\langle\varepsilon_2(E)\rangle]$ parts of the pseudodielectric function $\langle\varepsilon(E)\rangle=\langle\varepsilon_1(E)\rangle+i\langle\varepsilon_2(E)\rangle$ for GaP(001) treated in (a) 1 wt % and (b) 50 wt % HF solutions for $t=0$ (as-degreased) and 1 min, together with that for clean bare GaP (heavy solid lines). Vertical arrows indicate the positions of each critical point (E_0, E_1, E_0', and E_2).

were made on a commercial contact-angle measurement apparatus (Kyowa Interface Science Co., Ltd.). The PL measurements were carried out at 300 K using the 325-nm line of a He–Cd laser (Kimmon IK3302R-E) chopped at 329 Hz as the source of excitation.

III. RESULTS AND DISCUSSION

A. Spectroscopic ellipsometry

Figure 1 shows the pseudodielectric function spectra $\langle\varepsilon(E)\rangle=\langle\varepsilon_1(E)\rangle+i\langle\varepsilon_2(E)\rangle$ for a GaP(001) surface treated in (a) 1 wt % and (b) 50 wt % HF solutions for $t=1$ min, together with that obtained from an as-received sample ($t=0$ s). For comparison, the $\langle\varepsilon(E)\rangle$ spectrum for a clean, nearly flat GaP surface is shown by the bold solid lines.[21,22] One can see in Fig. 1 at least four critical points in the $\langle\varepsilon(E)\rangle$ spectra: E_0 (~2.76 eV), E_1 (~3.71 eV), E_0' (~4.74 eV), and E_2 (~5.28 eV). These critical points arise from singularities in the joint density of states.[23,24]

The imaginary part of the pseudodielectric function at the E_2 (or E_0') peak maximum, $\langle\varepsilon(E_2)\rangle$, is a sensitive and unambiguous indication of the sharpness of the dielectric discontinuity between the substrate and ambient. The SE measurement, therefore, can yield direct information about the relative quality of surface regions prepared by different methods. In Fig. 1, the $\langle\varepsilon(E_2)\rangle$ value slightly increases as the samples are immersed in the solutions, showing a value of $\langle\varepsilon(E_2)\rangle\sim 3$ for $t=1$ min, and keeps this value with further increase of immersion time up to 1 min (longest time we measured, not shown in Fig. 1).

To provide more quantitative information on the spectral difference of $\langle\varepsilon(E)\rangle$, we solved the Fresnel's equation under the assumption of a three-layer (ambient/overlayer/bulk GaP) model. An oxide overlayer or a roughened surface overlayer was taken into consideration. The native oxide or roughened overlayer thickness was numerically determined by minimizing the following mean-square deviation with a linear regression analysis (LRA) program[20]:

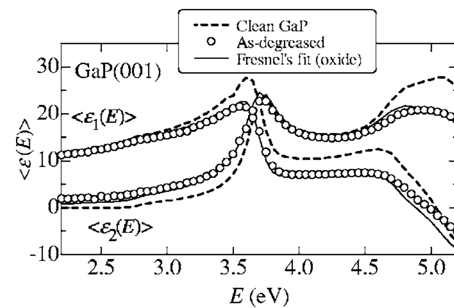

FIG. 2. Real $[\langle\varepsilon_1(E)\rangle]$ and imaginary $[\langle\varepsilon_2(E)\rangle]$ parts of the pseudodielectric function $\langle\varepsilon(E)\rangle=\langle\varepsilon_1(E)\rangle+i\langle\varepsilon_2(E)\rangle$ for an as-degreased GaP(001) sample. Dashed lines represent the $\langle\varepsilon(E)\rangle$ spectrum taken from a clean, nearly abrupt GaP surface. The result of the three-layer (ambient/native oxide overlayer/bulk GaP) model is shown by the solid lines. This analysis yields an apparent oxide thickness of $d_{ox}=1.95$ nm with an unbiased estimator of $\sigma=0.020$.

$$\sigma^2=\frac{1}{N-P-1}\sum_{i=1}^{N}\{(\tan\Psi_i^{exp}-\tan\Psi_i^{calc})^2+(\cos\Delta_i^{exp}-\cos\Delta_i^{calc})^2\}, \quad (1)$$

where N is the number of data points and P is the number of unknown parameters. The optical constants of GaP and its native oxide used in the analysis are taken from Refs. 21 and 22 (GaP) and from Refs. 25 and 26 (native oxide), respectively. Because of no experimental data on the optical constants of the native GaP oxide, we used the dielectric constants of the anodic GaP oxide formed in a diluted orthophosphoric acid/H_3PO_4 electrolyte.[25]

The solid lines in Fig. 2 show the analyzed results of the three-layer model with the native oxide as the overlayer for the as-degreased sample. The measured SE data are plotted by the open circles. The $\langle\varepsilon(E)\rangle$ spectrum taken for a clean, nearly abrupt GaP surface is also shown by the dashed lines. From this analysis, we obtain an apparent GaP oxide overlayer thickness of $d_{ox}=1.95$ nm with an unbiased estimator of $\sigma=0.020$.

The three-layer analysis result for a sample treated in 1 wt % HF solution for $t=1$ min is shown in Fig. 3(a) by the solid lines. The experimental SE $\langle\varepsilon(E)\rangle$ data are plotted by the open circles. The analysis yields an apparent GaP oxide film thickness of $d_{ox}=1.00$ nm with an unbiased estimator of $\sigma=0.012$.

Figure 4 plots the apparent oxide thickness d_{ox} obtained from the three-layer model versus immersion time t in 1 wt % and 50 wt % HF solutions. It is clear from Fig. 4 that removal of the native oxide is achieved by immersing the sample in the HF solutions. However, we never obtained a bare GaP surface (i.e., $d_{ox}\sim 0$ nm) even after enough etching. One possible reason for this is because our HF treatment indeed removes the native oxide and leaves a bare GaP surface, but as soon as the sample is brought out into the air to set on an SE goniometer a new oxide may start to grow during SE measurement ($\leq$5 min). A roughened surface overlying layer is also the cause of the reduction in $\langle\varepsilon(E)\rangle$ strength, thus providing $d_{ox}\neq 0$ nm.

To take account of the effect of a roughened surface overlayer, we used an effective medium approximation

Downloaded 11 Oct 2007 to 210.151.113.98. Redistribution subject to AIP license or copyright, see http://jap.aip.org/jap/copyright.jsp

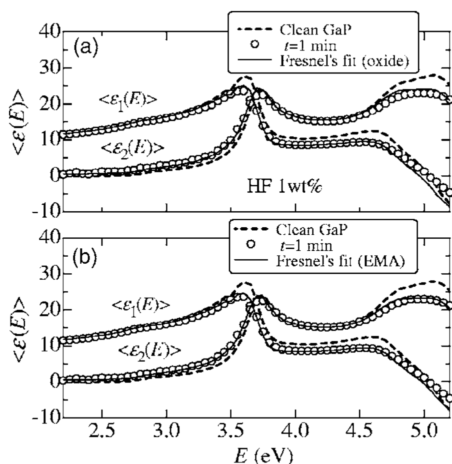

FIG. 3. (a) Real [$\langle \varepsilon_1(E) \rangle$] and imaginary [$\langle \varepsilon_2(E) \rangle$] parts of the pseudodielectric function $\langle \varepsilon(E) \rangle = \langle \varepsilon_1(E) \rangle + i \langle \varepsilon_2(E) \rangle$ for GaP(001) treated in 1 wt % HF solution for $t=1$ min. Solid lines show the calculated result of three-layer (ambient/native oxide overlayer/bulk GaP) model, which yields an apparent oxide thickness d_{ox} of 1.00 nm with $\sigma=0.009$. (b) As in (a), but the Bruggeman EMA–LRA result is shown by the solid lines. The bulk density deficit (f_v) and the roughness layer thickness obtained from this analysis are 65.0% and 0.98 nm, respectively, with $\sigma=0.009$.

(EMA) with the three-layer (ambient/roughened overlayer/bulk GaP) model while ignoring a possible thin oxide film. The EMA in this case deals with an overlayer consisting of two constituents: voids (density deficit; $\varepsilon_v=1+i0$) and bulk GaP (ε_c). We use the Bruggeman EMA (Ref. 27):

$$f_v \frac{\varepsilon_v - \varepsilon}{\varepsilon_v + 2\varepsilon} + f_c \frac{\varepsilon_c - \varepsilon}{\varepsilon_c + 2\varepsilon} = 0, \qquad (2)$$

$$f_v + f_c = 1, \qquad (3)$$

where f_v and f_c are the volume fractions of the voids and bulk GaP, respectively, and ε is the complex dielectric function of the effective medium assumed here. The unknown parameters were finally determined using the LRA program in Eq. (1).

The solid lines in Fig. 3(b) show the Bruggeman EMA result for a sample treated in 1 wt % HF solution for $t=1$ min. The bulk density deficit (f_v) and the roughened overlayer thickness determined here are 65.0% and 0.98 nm, respectively, with $\sigma=0.009$. We can see that the Bruggeman EMA (i.e., microroughness) gives nearly the same agreement with the oxide overlayer model given in Fig. 3(a). Because of a relatively thin overlayer (~1 nm, Fig. 3), however, we cannot successfully identify the actual structure of the GaP(001) surface, covered with either an oxide or a roughened overlayer, from only the SE modeling. We therefore used *ex situ* AFM to independently assess the NH_4OH-cleaned surface morphology.

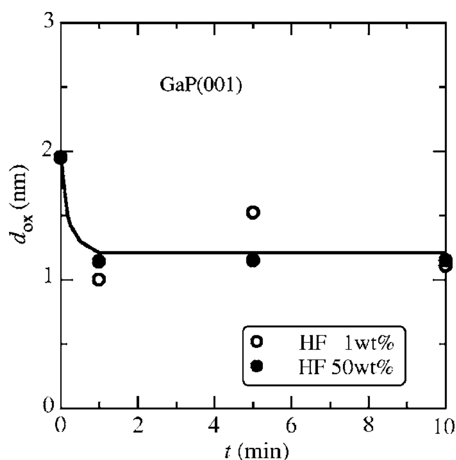

FIG. 4. Apparent native oxide thickness d_{ox} obtained from three-layer (ambient/native oxide overlayer/bulk GaP) model versus immersion time t for GaP(001) in 1 wt % and 50 wt % HF solutions.

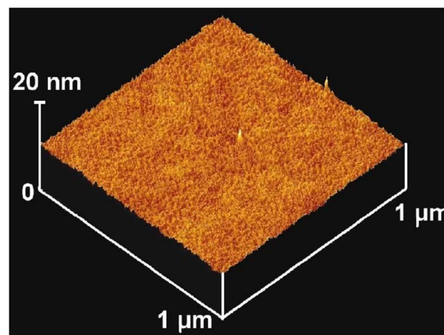

FIG. 5. (Color online) Large-area (1×1 μm^2) AFM image obtained from a sample treated in 1 wt % HF solution for $t=1$ min. The rms roughness obtained from this image is ~0.3 nm.

B. Atomic force microscopy

Figure 5 shows a large-area (1×1 μm^2) AFM image observed on a GaP(001) surface treated in 1 wt % HF solution for $t=1$ min. The root-mean-square (rms) roughness obtained from this image is 0.3 nm. This value is considerably smaller than that obtained from the Bruggeman-EMA roughness of ~1 nm in Fig. 3(b). We can thus conclude that the HF-etched GaP surface is covered with the native GaP oxide rather than the roughened overlayer. The AFM images also suggested that the GaP surface cannot be degraded so greatly by long-time immersion in the HF solution. This is in direct contrast to the case of HCl etching: an increase in the roughened overlayer thickness with increasing immersion time t in HCl was observed on GaP(111), GaAs(001), and InP(001) surfaces.[2,14,17] It should also be noted that the AFM roughness value derived from the HF-cleaned GaP surface, ~0.3 nm, is nearly the same as those obtained on the HF-cleaned GaAs and InP surfaces (~0.2–0.3 nm).[3,9]

C. X-ray photoelectron spectroscopy

The chemical composition of the GaP(001) surface before and after HF etching is characterized using XPS. The XPS survey spectra showed considerable amounts of oxygen species on the as-degreased surface. On the other hand, a small quantity of oxygen species was detected on the HF-etched GaP surface. Some of the oxygen species may be associated with gallium and phosphorous bonded to oxygen as in Ga_2O_3 and P_2O_5. Carbon contamination was also detected on both the as-degreased and HF-etched surfaces, which may be mainly due to adsorbed CO_2, CH_4, etc.

Downloaded 11 Oct 2007 to 210.151.113.98. Redistribution subject to AIP license or copyright, see http://jap.aip.org/jap/copyright.jsp

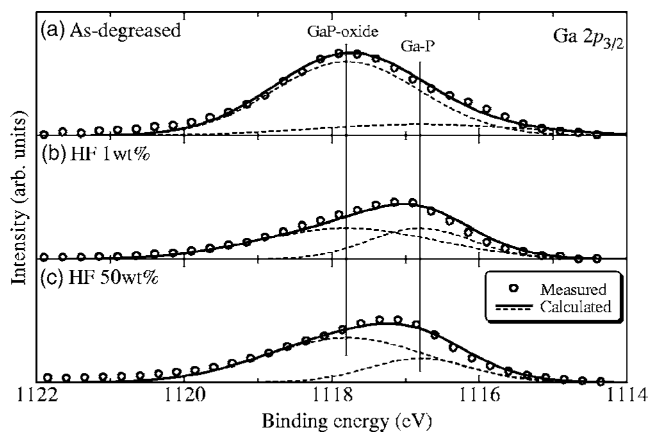

FIG. 6. XPS spectra in the Ga $2p_{3/2}$ region for (a) as-degreased, (b) 1 wt % HF-etched, and (c) 50 wt % HF-etched samples (t=1 min).

Figure 6 shows the XPS spectra in the Ga $2p_{3/2}$ region for the as-degreased sample, together with those etched in 1 wt % and 50 wt % HF solutions for t=1 min. The main peaks in Fig. 6(a) at ~1117 and ~1118 eV are, respectively, due to the Ga−P bond and the GaP oxide (Ga_2O, Ga_2O_3, etc.).[28] We can conclude from Fig. 6 that the HF etching removes the native GaP oxide; however, complete removal of the oxide cannot be achieved even after longer etching. This may be due to the fact that the HF etching can remove the native GaP oxide and leave a bare GaP surface, but as soon as the sample is exposed to air, an oxide regrowth starts to occur. The air-exposure time dependence of the oxide film thickness on the GaP(111)A surface was reported to exhibit a logarithmic behavior, yielding an oxide growth of about 0.3–0.4 nm/decade.[17]

Figure 7 shows the XPS spectra in the P $2p$ region for the as-degreased sample, together with those etched in 1 wt % and 50 wt % HF solutions for t=1 min. The P $2p$ peak at ~130 eV can be deconvoluted into the two peaks P $2p_{3/2}$ and P $2p_{1/2}$, with a peak energy difference of ~0.9 eV. The binding energy of the native oxide is seen at energy about 5 eV higher than that of the P $2p$ core level. The XPS spectra shown in Fig. 7 also verify the native oxide removal by HF etching, but suggest the presence of a newly grown oxide film on the etch-cleaned surface. To obtain better

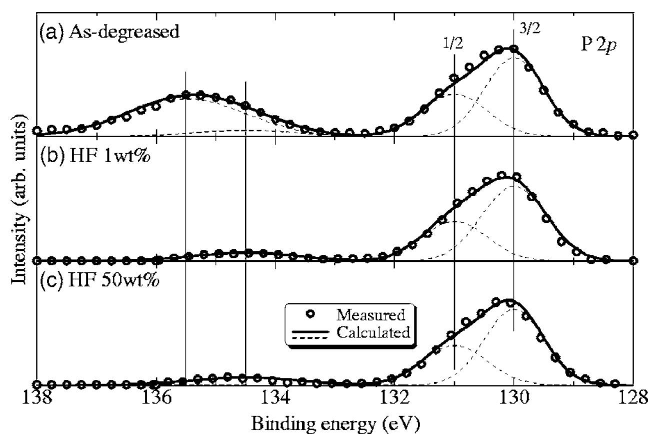

FIG. 7. XPS spectra in P $2p$ region for (a) as-degreased, (b) 1 wt % HF-etched, and (c) 50 wt % HF-etched samples (t=1 min).

agreement with the experimental data, we considered an unidentified peak at ~134.5 eV. The origin of this peak is not clear at present, but we consider that it arises from GaP oxides.

The native oxide thickness d_{ox} can be estimated from the measured XPS intensity of oxide, I_{ox}, and of GaP, I_{GaP}, by the following expression[29]:

$$d_{ox} = \lambda_{ox} \cos \theta \ln\left(\frac{I_{ox}\rho_{GaP}\lambda_{GaP}M_{ox}}{I_{GaP}\rho_{ox}\lambda_{ox}M_{GaP}} + 1\right), \quad (4)$$

where θ is the take-off angle (45°), λ_{GaP} and λ_{ox} are, respectively, inelastic mean free paths of the photoelectrons in GaP and its oxide, ρ_{GaP} and ρ_{ox} are the densities of GaP and its oxide, respectively, and M_{GaP} and M_{ox} are the molecular weights of GaP and its oxide, respectively.

No detailed experimental data have been reported on λ_{GaP} and λ_{ox} to date. We therefore use the values of λ_{GaP} =0.8 nm and λ_{ox}=0.4 nm, where the GaP value is obtained by Gergely *et al.*[30] Introducing these λ values into Eq. (4), we obtain an oxide layer thicknesses of d_{ox}~2.1 nm [Fig. 7(a)], ~0.6 nm [Fig. 7(b)], and ~0.6 nm [Fig. 7(c)], respectively. It should be noted that the as-degreased oxide value d_{ox}~2.1 nm is in good agreement with that obtained from the SE data analysis (d_{ox}~2.0 nm, Fig. 4). We must note, however, that our present XPS analyses have not enough accuracy. This is because the chemical structure of the oxide in the etched samples is obviously different from that of the as-degreased sample as indicated in Fig. 7, which presumably causes the change in the mean free path and materials density. Furthermore, the evaluation of the oxide thickness is done in angle-resolved mode to obtain an appropriate accuracy.

As mentioned before, the oxide thickness d_{ox} in Fig. 4 corresponds to the equivalent modeled dielectric layer thickness of the GaP oxide, including the effect of surface microroughness. From the apparent oxide thickness d_{ox}~1 nm derived in Fig. 4 (t=1 min) and the AFM rms roughness value ~0.3 nm, we can obtain the native GaP oxide thickness of the HF-cleaned surface to be ~0.7 nm. This value is in reasonable agreement with that obtained from the XPS analysis, ~0.6 nm (Fig. 7).

D. Wettability

Wettability measurement is a very surface-sensitive technique that has been previously shown to be able to detect changes in semiconductor surfaces.[2–7,31,32] A straightforward method to determine wettability is to measure the contact angle of a drop of water on the surface. If the wettability is high, the contact angle θ will be small and the surface hydrophilic. On the contrary, if the wettability is low, θ will be large and the surface hydrophobic.

We plot in Fig. 8 the contact angle θ measured on GaP(001) versus immersion time t in 1 wt % and 50 wt % HF solutions. As mentioned before, the starting samples used here were covered with native oxide. The contact angle measured for this sample (t=0 min) is ~50°. As seen in Fig. 8, θ increased rapidly with increasing t and then showed a saturated value of ~70°.

Downloaded 11 Oct 2007 to 210.151.113.98. Redistribution subject to AIP license or copyright, see http://jap.aip.org/jap/copyright.jsp

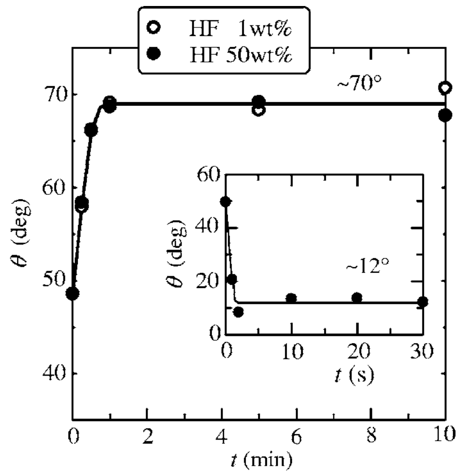

FIG. 8. Plots of the contact angle θ versus immersion time t in 1 wt % and 50 wt % HF solutions. Results of GaP(001) immersed in aqueous alkaline (NH_4OH) solution are shown in the inset (Ref. 18).

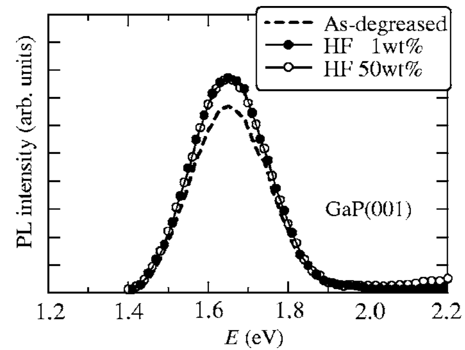

FIG. 9. PL peak spectra at ~1.65 eV measured at 300 K for GaP(001) treated in 1 wt % and 50 wt % HF solutions for t=1 min, together with that obtained from the as-degreased sample.

Matsushita *et al.*[33] studied ($H_2SO_4/H_2O_2/H_2O$)-, HC1-, and HF-treated GaAs surfaces by means of contact angle measurements. They reported that such acid-cleaned GaAs surfaces are hydrophobic. It is also shown that the HCl- and HF-treated GaAs and InP surfaces are hydrophobic.[2,3,9,14] These results are in direct contrast to those obtained on alkaline-etched GaP(001) surfaces (i.e., hydrophilic). The inset in Fig. 8 shows the NH_4OH-etched GaP(001) data taken from Ref. 18. The NH_4OH-etched GaP(001) surface is found to be hydrophilic ($\theta \sim 12°$). It was also reported that the alkaline-etched GaAs(001) surfaces are hydrophilic ($\theta \sim 25°$).[5]

Hydrophilicity and hydrophobicity are related to the existence of certain surface chemical species.[34,35] The origin of hydrophilicity is attributed to singular and associated hydroxyl groups on the GaP and GaAs surfaces, while the hydrophobic surfaces on acid- (HF- and HCl-) treated surfaces may be mainly characterized by the H- (Cl-) terminated surfaces. In III−V semiconductors, the concentrated HCl solution is well known to produce stable, Cl-terminated surfaces.[4]

E. Photoluminescence

PL spectroscopy can be used as a tool for the study of the electronic surface properties of semiconductors.[36–39] Nonradiative recombination at the surface has been phenomenologically taken into consideration by the concept of surface recombination velocity. We measured the 300-K PL spectra to obtain information on the surface properties of GaP(001) before and after HF etching.

Figure 9 shows the 1.65-eV PL peak measured for GaP(001) treated in 1 wt % and 50 wt % HF solutions for t =1 min, together with that obtained from the as-degreased sample. Note that the as-degreased sample has a native oxide overlayer (~1 nm), whereas the HF-etched samples have a very thin native oxide overlayer. It can be understood from Fig. 9 that the PL intensity slightly increases after etching in the HF solutions.

In case of the HCl etching of GaP (111)A,[17] a large decrease of the PL intensity was observed after HCl treatment; i.e., the 1.65-eV PL peak intensity decreased to about 20% by the HCl etching. The surface recombination velocity is the only parameter required to characterize the surface. The weaker PL intensity after HCl cleaning was, thus, considered to be due to the increase in the surface recombination velocity caused by the native GaP oxide removal. It is possible to consider that the slight increase in the PL intensity observed in the HF-cleaned GaP(001) surface is due to surface hydrogen passivation. However, further study is needed to judge this consideration.

IV. CONCLUSIONS

SE, *ex situ* AFM, XPS, contact-angle, and PL measurements were carried out to obtain information about GaP(001) surfaces treated in aqueous HF (1 wt % and 50 wt %) solutions. The SE data clearly indicated that HF solutions cause the removal of the native GaP oxide immediately upon immersing the sample in the solutions. The XPS data confirmed the removal of the native oxide from the GaP surface. A Bruggeman EMA−LRA simulation suggested the presence of a roughened overlayer ~1 nm thick on the HF-cleaned surface, while the AFM roughness (rms) value was ~0.3 nm. The AFM value obtained here was found to be nearly the same as those derived on HF-cleaned GaAs and InP surfaces (~0.2–0.3 nm). The XPS data further suggested an oxide overlayer even on the HF-etched GaP surface. The contact-angle measurements indicated that the HF-cleaned surface is hydrophobic, which is in direct contrast to those obtained from NH_4OH-cleaned surfaces (hydrophilic). The PL emission intensity was also found to slightly increase by etching in the HF solutions.

ACKNOWLEDGMENTS

The authors thank Dr. M. Yokogawa, Dr. T. Nishiura, Dr. A. Hachigou, Professor T. Miyazaki, and Professor S. Ozaki for their helpful discussions.

[1]S. I. Ingrey, in *Handbook of Compound Semiconductors*, edited by P. H. Holloway and G. E. McGuire (Noyes, NJ, 1995).
[2]S. Osakabe and S. Adachi, Jpn. J. Appl. Phys., Part 1 **36**, 7119 (1997) (and references therein.).

Downloaded 11 Oct 2007 to 210.151.113.98. Redistribution subject to AIP license or copyright, see http://jap.aip.org/jap/copyright.jsp

[3] D. Kikuchi and S. Adachi, Mater. Sci. Eng., B **76**, 133 (2000) (and references therein).
[4] Z. H. Lu, F. Chatenoud, M. M. Dion, M. J. Graham, H. E. Ruda, I. Koutzarov, Q. Lin, C. E. J. Mitchell, I. G. Hill, and A. B. McLean, Appl. Phys. Lett. **67**, 670 (1995).
[5] S. Osakabe and S. Adachi, J. Electrochem. Soc. **144**, 290 (1997).
[6] P. Schmuki, G. I. Sproule, J. A. Bardwell, Z. H. Lu, and M. J. Graham, J. Appl. Phys. **79**, 7303 (1996).
[7] Z. H. Lu, T. Tyliszczak, and A. P. Hitchcock, Phys. Rev. B **58**, 13820 (1998).
[8] O. E. Tereshchenko, S. I. Chikichev, and A. S. Terekhov, J. Vac. Sci. Technol. A **17**, 2655 (1999).
[9] S. Adachi and D. Kikuchi, J. Electrochem. Soc. **147**, 4618 (2000).
[10] Z. Liu, Y. Sun, F. Machuca, P. Pianetta, W. E. Spicer, and R. F. W. Pease, J. Vac. Sci. Technol. A **21**, 212 (2003).
[11] Z. Liu, Y. Sun, F. Machuca, P. Pianetta, W. E. Spicer, and R. F. W. Pease, J. Vac. Sci. Technol. B **21**, 1953 (2003).
[12] V. L. Alperovich, O. E. Tereshchenko, N. S. Rudaya, D. V. Sheglov, A. V. Latyshev, and A. S. Terekhov, Appl. Surf. Sci. **235**, 249 (2004).
[13] T. Mayer, M. V. Lebedev, R. Hunger, and W. Jaegermann, J. Phys. Chem. B **110**, 2293 (2006).
[14] D. Kikuchi, Y. Matsui, and S. Adachi, J. Electrochem. Soc. **147**, 1973 (2000).
[15] O. Pluchery, Y. J. Chabal, and R. L. Opila, J. Appl. Phys. **94**, 2707 (2003).
[16] Y. Sun, Z. Liu, F. Machuca, P. Pianetta, and W. E. Spicer, J. Appl. Phys. **97**, 124902 (2005).
[17] K. Tomioka and S. Adachi, J. Electrochem. Soc. **152**, G173 (2005).
[18] H. Morota and S. Adachi, J. Appl. Phys. **100**, 054904 (2006).
[19] A. R. Clawson, Mater. Sci. Eng., R **31**, 1 (2001).
[20] R. M. A. Azzam and N. M. Bashara, *Ellipsometry and Polarized Light* (North-Holland, Amsterdam, 1977).
[21] G. E. Jellison, Jr., Opt. Mater. **1**, 151 (1992).
[22] S. Adachi, *Optical Constants of Crystalline and Amorphous Semiconductors: Numerical Data and Graphical Information* (Kluwer Academic, Boston, 1999).
[23] S. Zollner, M. Garriga, J. Kircher, J. Humlíček, M. Cardona, and G. Neuhold, Phys. Rev. B **48**, 7915 (1993).
[24] S. Adachi, *Properties of Group-IV, III−V and II−VI Semiconductors* (Wiley, Chichester, 2005).
[25] D. E. Aspnes, B. Schwartz, A. A. Studna, L. Derick, and L. A. Koszi, J. Appl. Phys. **48**, 3510 (1977).
[26] S. Zollner, Appl. Phys. Lett. **63**, 2523 (1993).
[27] M. Erman, J. B. Theeten, P. Chambon, S. M. Kelso, and D. E. Aspnes, J. Appl. Phys. **56**, 2664 (1984).
[28] C. C. Surdu-Bob, S. O. Saied, and J. L. Sullivan, Appl. Surf. Sci. **183**, 126 (2001).
[29] N. Tomita and S. Adachi, Jpn. J. Appl. Phys., Part 1 **40**, 6705 (2001).
[30] G. Gergely, M. Menyhard, S. Gurban, Z. Benedek, C. Daroczi, V. Rakovics, J. Tóth, D. Varga, M. Krawczyk, and A. Jablonski, Surf. Interface Anal. **30**, 195 (2000).
[31] L. Li, H. Bender, G. Zou, P. W. Mertens, M. A. Meuris, and M. M. Heyns, J. Electrochem. Soc. **143**, 233 (1996).
[32] I.-M. Lee and C. G. Takoudis, J. Vac. Sci. Technol. A **15**, 3154 (1997).
[33] K. Matsushita, S. Miyazaki, S. Okuyama, and Y. Kumagai, Jpn. J. Appl. Phys., Part 1 **33**, 4576 (1994).
[34] Y. Bäcklund, K. Hermansson, and L. Smith, J. Electrochem. Soc. **139**, 2299 (1992).
[35] M. Grundner and H. Jacob, Appl. Phys. A **39**, 73 (1986).
[36] K. Mettler, Appl. Phys. **12**, 75 (1977).
[37] R. E. Hollingsworth and J. R. Sites, J. Appl. Phys. **53**, 5357 (1982).
[38] W. S. Hobson and A. B. Ellis, J. Appl. Phys. **54**, 5956 (1983).
[39] A. A. Burk, Jr., P. B. Johnson, W. S. Hobson, and A. B. Ellis, J. Appl. Phys. **59**, 1621 (1986).

Downloaded 11 Oct 2007 to 210.151.113.98. Redistribution subject to AIP license or copyright, see http://jap.aip.org/jap/copyright.jsp